# Viscous Shock-Layer Flows for the Space Shuttle Windward Plane of Symmetry

E. Wade Miner* and Clark H. Lewis†
*Virginia Polytechnic Institute and State University, Blacksburg, Va.*

**A finite-difference viscous shock-layer method is applied to the problem of predicting hypersonic viscous shock-layer flows over nonanalytic blunt bodies at re-entry conditions such as the windward plane of symmetry of the space shuttle orbiter. The present predictions agreed well with the boundary-layer predictions of Tong, Buckingham and Morse for a shuttle orbiter configuration at 224,000 ft. The present predictions for a 4-ft nose radius, 20° sphere cone at 280,000 and 310,000 ft showed the correct altitude effects and appeared entirely reasonable. The present results for these cases indicate the validity of using the present viscous shock-layer method for predicting the space shuttle windward plane of symmetry flowfield at re-entry conditions.**

## Nomenclature

$C_i$ = concentration of species $i, \rho_i/\rho$
$C_p$ = specific heat at constant pressure
ECW = denotes equilibrium catalytic wall
FVSL = denotes fully viscous shock layer
$h$ = static enthalpy, $h^*/U_\infty{}^{*2}$
$J_i$ = diffusion mass flux of species $i, (-\mu/Pr)Le_i \partial C_i/\partial y$
$k$ = thermal conductivity, $k^*/(\mu^*_{\text{ref}} C^*_{p\infty})$
$\text{Le}_i$ = Lewis number, $C^*_p \rho^* D^*_i/k^*$
$M$ = molecular weight
$M_\infty$ = freestream Mach number
$\bar{M}$ = mixture molecular weight, $1/(\sum_i C_i/M_i)$
$N_e$ = number of electrons/cm$^3$
NCW = denotes noncatalytic wall
$P$ = pressure, $P^*/(\rho^*_\infty U^{*2}_\infty)$
$Pr$ = Prandtl number $C^*_p \mu^*/k^*$
$q$ = heat transfer, $q^*/(\rho^*_\infty U^{*3}_\infty)$
$r$ = body radius, $r^*/R^*_n$
$R$ = universal gas constant
$R^*_n$ = body nose radius
$Re_\infty/\text{ft}$ = freestream Reynolds number per foot, $\rho^*_\infty U^*_\infty/\mu^*_\infty$
$Re_\infty/\text{m}$ = freestream Reynolds number per meter, $\rho^*_\infty U^*_\infty/\mu^*_\infty$
$s$ = coordinate measured along body surface, $s^*/R^*_n$
St = Stanton number, $q_w/(H_\infty - H_w)$
SS = denotes shock slip
$t$ = time from shuttle orbiter reentry
$T$ = temperature, $T^*/T^*_{\text{ref}}$
$T^*_{\text{ref}}$ = reference temperature, $U^{*2}_\infty/C^*_{p\infty}$
TVSL = denotes thin viscous shock layer
$u$ = velocity component tangent to the body surface, $u^*/U^*_\infty$
$U^*_\infty$ = freestream velocity
$v$ = velocity component normal to the body surface, $v^*/U^*_\infty$
$\dot{w}_i$ = production term for species $i, \dot{w}^*_i R^*_n/\rho^*_\infty U^*_\infty$
$y$ = coordinate measured normal to the body, $y^*/R^*_n$
$z$ = coordinate measured along body axis, $z^*/R^*_n$
$\epsilon$ = Reynolds number parameter, $[\mu^*_{\text{ref}}/\rho^*_\infty U^*_\infty R_n{}^*]^{1/2}$
$\theta_c$ = cone half angle, deg
$\kappa$ = surface curvature, $\kappa^* R^*_n$
$\mu$ = coefficient of viscosity, $\mu^*/\mu^*_{\text{ref}}$
$\mu^*_{\text{ref}}$ = coefficient of viscosity evaluated at $T^*_{\text{ref}}$
$\rho$ = density, $\rho^*/\rho^*_\infty$
$\phi$ = angle between body tangent and axis

*Superscripts*

$j$ = indicator for axisymmetric flow (1) or two-dimensional flow (0)
$*$ = dimensional quantities

*Subscripts*

$i$ = species $i$
sh = value behind the shock
0 = stagnation point value
$\infty$ = freestream value
$w$ = wall value

Presented as Paper 74-756 at the AIAA/ASME 1974 Thermophysics and Heat Transfer Conference, Boston, Mass., July 15-17, 1974; submitted February 13, 1975; revision received May 19, 1975. This research was supported by NASA Contract NAS9-12630 and the Smithsonian Institution.

Index categories: Viscous Nonboundary-Layer Flows; Reactive Flows; Supersonic and Hypersonic Flow.

*Currently, Curator, Department of Science and Technology, National Air and Space Museum, Smithsonian Institution, Washington, D.C. Member AIAA.

†Professor, Aerospace and Ocean Engineering Department. Associate Fellow AIAA.

## Introduction

THE current development program for the space shuttle has stimulated considerable interest in techniques for predicting the hypersonic flowfields over bodies such as the re-entering space shuttle orbiter. So far, much of the work which has been done has been limited to the inviscid flowfield, for example, the work of Kutler, Warming, and Lomax[1] and Kutler, Reinhardt, and Warming.[2] While the inviscid flowfield is of considerable interest to the vehicle designers, the viscous flowfield is of great importance. Predictions of viscous flowfields for the shuttle windward plane of symmetry have been made with a boundary-layer method by Tong, Buckingham, and Morse.[3] In terms of the space shuttle trajectory, the use of a boundary-layer approach is more appropriate to the lower altitude points of the trajectory, i.e., to supersonic high Reynolds number flows in which the boundary layer is thin compared to the shock-layer thickness. At the higher altitudes of the space shuttle trajectory, boundary-layer theory becomes increasingly inadequate as the Reynolds number decreases. For example, at hypersonic, low Reynolds number conditions, the viscous layer may extend to the shock, especially in the stagnation region. In such a case, the boundary-layer assumptions would not be appropriate.

Viscous shock-layer methods can be applied at much higher altitudes than can boundary-layer methods. The entire flowfield from the body to the shcok is treated in a unified manner in the viscous shock-layer methods, and it is not necessary to assume that the viscous effects are confined to a thin layer near the body surface. A thin viscous shock-layer (TVSL) method was used by Tong, Buckingham, and Morse,[3] but only for the stagnation streamline flow.

Methods have been developed for applying TVSL theory away from the stagnation streamline. An example is the integral method of Kang and Dunn.[4-7] This method was applied to flows over spherically blunted cones, including a 20° sphere cone with $R_n^* = 4$ ft as approximating the space shuttle windward plane of symmetry. Many other researchers have been involved in developing viscous shock-layer methods. Among these researchers, Davis[8-9] achieved a significant degree of success. The major advantages of the methods of Davis were the ease and speed with which solutions far downstream could be obtained.

The authors of this paper have previously developed a finite-difference method for predicting hypersonic, nonequilibrium viscous shock-layer flows over nonanalytic blunt bodies.[10] This method could be applied to the downstream portion of the flowfield as well as on the stagnation streamline. It was also second-order accurate in the Reynolds number parameter $\epsilon$ from the body to the shock, and it could be used for fully viscous shock-layer (FVSL) flows as well as for TVSL flows. The method of Ref. 10 was similar in problem formulation and solution procedure to the methods of Davis,[8-9] but differed in several respects, viz: a) the body geometries were not restricted to analytic shapes such as the hyperboloids Davis considered for which the pressure distributions were nearly Newtonian, b) the initial shock shape could differ from the body shape (as for sphere cones), and c) the chemistry was for a multicomponent mixture of reacting gases. Thus, the method of Ref. 10 should be well suited to the problem of predicting the viscous flowfield for the windward plane of symmetry of the space shuttle orbiter.

In the present work, the viscous shock-layer equations were solved for flows over two bodies which approximate the space shuttle windward plane of symmetry. Predictions of the present method are compared with the predictions of the boundary-layer method of Tong, Buchingham, and Morse[3] for a space shuttle windward plane of symmetry configuration at 224,000 ft, and with the results which Kang and Dunn[4-7] obtained with a more approximate integral method for a 20° sphere cone at 280,000 and 310,000 ft.

## Theoretical Model

In the present work, the governing equations for hypersonic viscous shock-layer flows are as given in Ref. 10. The equations apply to axisymmetric or two-dimensional flows and are accurate to the second order in terms of the Reynolds number parameter $\epsilon$ from the body to the shock. Both longitudinal and transverse curvatures are included. The coordinate system is shown in Fig. 1. For a multicomponent mixture of reacting gases, the governing equations are

Continuity Equation

$$(\partial/\partial s)\,[\,(r+y\cos\phi)^j \rho u\,] + (\partial/\partial y)\,[\,(1+\kappa y)\,(r+y\cos\phi)^j \rho v\,] = 0 \tag{1}$$

S-Momentum Equation

$$\frac{1}{1+\kappa y}\rho u\frac{\partial u}{\partial s} + \rho v\frac{\partial u}{\partial y} + \rho uv\frac{\kappa}{1+\kappa y} + \frac{1}{1+\kappa y}\frac{\partial P}{\partial s} = \epsilon^2\frac{\partial}{\partial y}\left[\mu\left(\frac{\partial u}{\partial y} - \frac{\kappa u}{1+\kappa y}\right)\right] + \epsilon^2\mu\left(\frac{2\kappa}{1+\kappa y} + \frac{j\cos\phi}{r+y\cos\phi}\right)\left(\frac{\partial u}{\partial y} - \frac{\kappa u}{1+\kappa y}\right) \tag{2}$$

Y-Momentum Equation

$$\partial P/\partial y = (\kappa/1+\kappa y)\,\rho u^2 - (1/1+\kappa y)\,\rho u(\partial v/\partial s) - \rho v(\partial v/\partial y) \quad \text{(FVSL)} \tag{3a}$$

which becomes

$$\partial P/\partial y = (\kappa/1+\kappa y)\,\rho u^2 \quad \text{(TVSL)} \tag{3b}$$

if the thin shock-layer approximation is made.

Energy Equation

$$\frac{1}{1+\kappa y}\rho u C_p\frac{\partial T}{\partial s} + \rho v C_p\frac{\partial T}{\partial y} - \frac{1}{1+\kappa y}u\frac{\partial P}{\partial s} - v\frac{\partial P}{\partial y} = \epsilon^2\frac{\partial}{\partial y}\left(k\frac{\partial T}{\partial y}\right) + \epsilon^2\left(\frac{\kappa}{1+\kappa y} + \frac{j\cos\phi}{r+y\cos\phi}\right)k\frac{\partial T}{\partial y} - \epsilon^2\sum_{i=1}^{ns} J_i C_{p_i}\frac{\partial T}{\partial y} + \epsilon^2\mu\left(\frac{\partial u}{\partial y} - \frac{\kappa u}{1+\kappa y}\right)^2 - \sum_{i=1}^{ns} h_i\dot{w}_i \tag{4}$$

Species Conservation Equations

$$\frac{1}{1+\kappa y}\rho u\frac{\partial C_i}{\partial s} + \rho v\frac{\partial C_i}{\partial y} = \dot{w}_i - \epsilon^2\frac{\partial}{\partial y}(J_i) - \epsilon^2\left(\frac{\kappa}{1+\kappa y} + \frac{j\cos\phi}{r+y\cos\phi}\right)J_i \tag{5}$$

where $J_i$ is the diffusion mass flux term of species $i$, and Equation of State

$$P = \rho RT/\bar{M}C^*_{p\infty} \tag{6}$$

The boundary conditions, transformation of equations, and solution procedure are as given in Ref. 10, except for the geometry for the space shuttle windward plane of symmetry. For the shuttle case, the body geometry was input to the computer program in tabular form of $s$, $r$, and $z$. A four-point walking least squares log-log curve fit was used to compute the first and second derivatives of $r$ with respect to $z$. From these derivatives, the surface curvature was calculated from the expression

$$\kappa = |d^2r/dz^2|\,\{1+(dr/dz)^2\}^{-1.5} \tag{7}$$

which is equivalent to the expression

$$\kappa = [\,(d^2r/ds^2)^2 + (d^2z/ds^2)^2\,]^{1/2} \tag{8}$$

In the present work the viscosity, thermal conductivity, and reaction rate data for the binary gas viscous shock-layer predictions were the same as those used by Davis,[8,9] while the thermodynamic data were from Browne.[11,12] For the multicomponent, viscous shock-layer predictions, the ther-

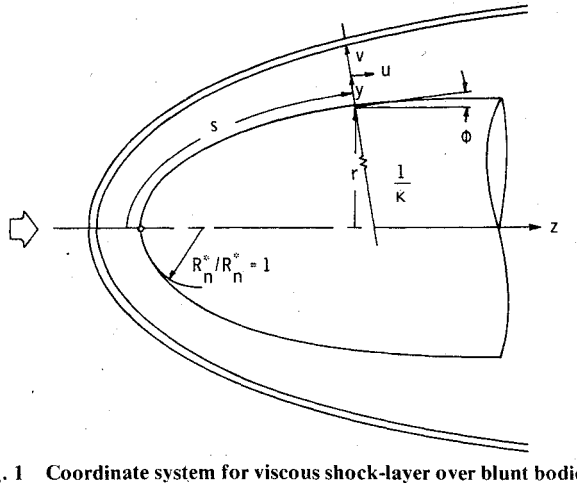


**Fig. 1 Coordinate system for viscous shock-layer over blunt bodies.**

modynamic data were from Browne[11-13] and the transport and reaction rate data were those given by Blottner.[14]

More complete details of the solution procedure and the finite-difference method are given in Ref. 15. The corresponding computer program is described in detail in Ref. 16, along with listings of the input and output data for sample cases.

## Results and Discussion

Predictions of the present viscous shock-layer method have previously been compared with the results of other numerical methods and with experimental data. Essentially exact agreement was obtained with the results of Davis[9] for a 10° hyperboloid at 225,000 ft. Good agreement was obtained with predictions of the finite-difference methods of Refs. 17-21 for the RAM C re-entry body at 230,000 ft and with the experimental electron concentration profiles given in Ref. 21 for the RAM C at 230,000 ft and other altitudes. Also, quite reasonable agreement was obtained with the experimental heat-transfer data of Pappas and Lee[22] for a 7.5° sphere cone at hypervelocity conditions. While these comparisons are not shown here, they have been presented in Refs. 10 and 15, and should further indicate the accuracy of the present method.

Predictions are presented here for hypersonic viscous shock-layer flows over two nonanalytic blunt bodies. In the first case, the geometry considered was the windward plane of symmetry of a space shuttle orbiter with $R_n^* = 2.667$ ft at 224,000 ft altitude, $U_\infty = 21{,}800$ fps and a 34° angle of attack. Under these conditions, the flowfield is near the upper limit of the boundary-layer regime, and this case provides a good comparison between the predictions of the present method and the predictions of the boundary-layer method of Tong, Buckingham, and Morse.[3] In the second case, the geometry considered is a 20° sphere cone with $R_n^* = 4$ ft at altitudes of 280,000 and 310,000 ft and at $U_\infty = 25{,}000$ fps. Under these conditions, the flowfield is within the viscous shock-layer regime and cannot be adequately treated with boundary-layer methods. This case was considered by Kang and Dunn[4-7] as approximating the windward plane of symmetry of the space shuttle orbiter.

### NASA Shuttle Geometry Case

The case considered by Tong, Buckingham, and Morse[3] was a space shuttle orbiter geometry using the Rockwell Shuttle 2007 trajectory at altitudes between 300,000 and 180,000 ft. They considered the windward plane of symmetry, and boundary-layer theory was used to predict the flow over the equivalent axisymmetric body. In Ref. 3 the body geometry was specified by a series of polynomial curve fits, which were faired into a cone of half-angle corresponding to the angle of attack. The geometry considered herewith followed the approach of Tong, but difficulties were encountered in directly using the polynomial curve fits for the forward portion of the body. In fact, the surface curvature as calculated from the polynomials was not only discontinuous but also changed sign. The polynomial curve fits were replaced by a table of $s$, $r$, and $z$ values, and a four-point walking least squares log-log curve fit was used to interpolate for the values of $r$ and $z$ corresponding to $s$ in this table. This approach gave a smooth, continuous distribution of surface curvature. The body geometry and the corresponding shock predicted by the present method are shown in Fig. 2 for $t = 800$ sec from re-entry at an altitude of 224,000 ft. Predictions by the present method were made for this particular case, since for the space shuttle at 224,000 ft both the first-order boundary-layer theory used by Tong and the viscous shock-layer theory used here should be equally appropriate.

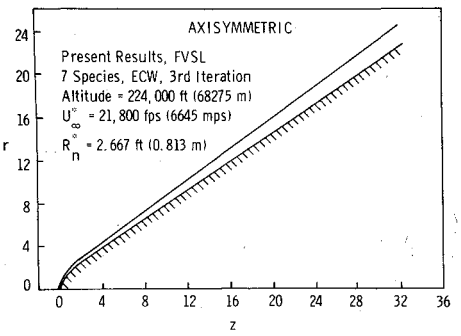


Fig. 2 Body and shock geometry for NASA shuttle-like body.

The pressure distribution predicted by the present method for $t = 800$ sec is shown in Fig. 3 with pressure distributions from Ref. 3, which were obtained with the tangent-cone approach. Results from the two methods agreed quite well.

Mass-fraction profiles at the stagnation point are compared in Fig. 4. Even though there was no attempt made to match the reaction rate data used in the present method with Tong's, the present results agreed reasonably well with his results. The most apparent differences were in the N profiles near the surface. Tong's results showed a pronounced rise in the N profile from the wall and then a gradual decrease, with a sharp decrease near the shock. The N profile predicted by the present method showed a slight increase near the wall and then a decrease near the shock similar to that of the N profile of Tong. The O profiles were quite similar. The present method predicted a slightly more rapid decrease in the outer portion of the flowfield. The NO profiles were also quite similar. The present method predicted a higher peak value of NO slightly farther from the shock. In considering the dif-

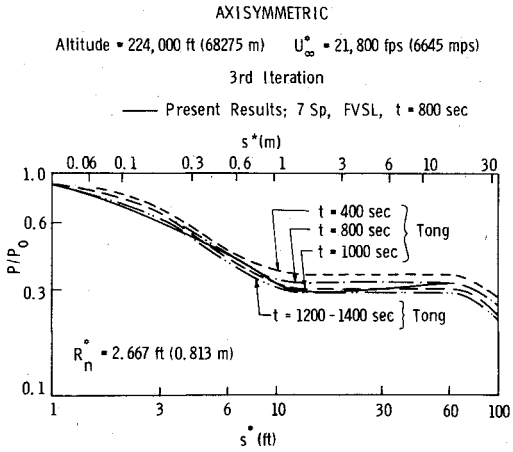


Fig.3 Pressure distributions for NASA shuttle-like body.

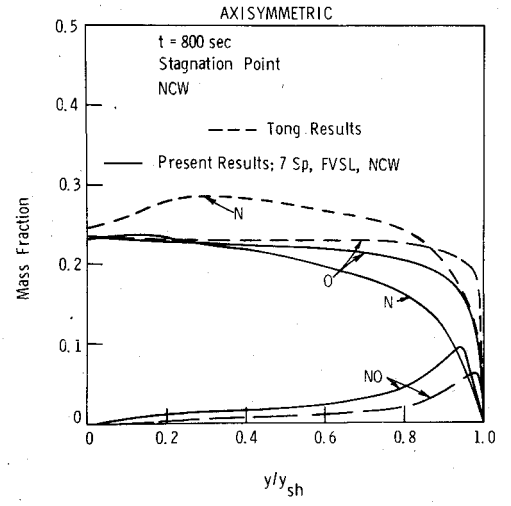


Fig. 4 Stagnation point species mass fractions for NASA shuttle-like body.

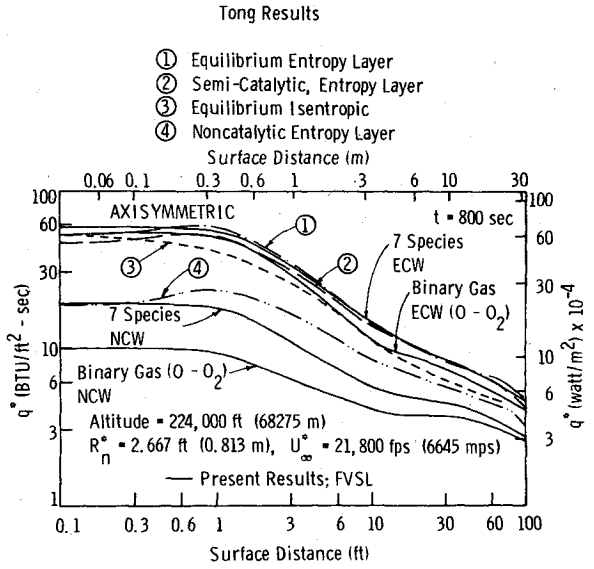


**Fig. 5 Heat-transfer distributions for NASA shuttle-like body.**

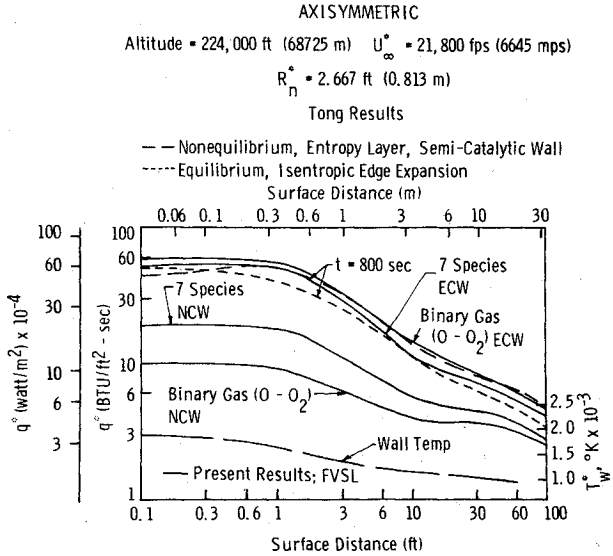


**Fig. 6 Heat-transfer and wall temperature distributions for NASA shuttle-like body.**

ference between the present results and the results of Tong, it should be noted that, not only were the reaction rates different but also the present results were FVSL, and the Tong results, at the stagnation point only, were TVSL. Considering these differences, the agreement between the present predictions and the predictions of Tong[3] is quite good.

While mass-fraction profile differences did exist, there was little difference in the predicted stagnation point hear transfer, as shown in the next figures. Heat-transfer distributions are shown in Figs. 5 and 6 and the wall temperature distribution is shown in Fig. 6. The predictions of the present method for the noncatalytic wall (NCW) condition showed a strong dependence on the gas model used. Over the forward portion of the body, the heat transfer for non-equilibrium air (seven species) was as much as twice that for dissociating oxygen. This difference decreased downstream. For the equilibrium catalytic wall (ECW) condition, there was little difference between the predictions of the present method for nonequilibrium air and dissociating oxygen. For both the ECW and the NCW conditions the present multicomponent gas results agreed well with the results of Tong, but the present method did not predict the rise in heat transfer at $s^* = 1$ ft, which Tong predicted when entropy-layer swallowing was included. It should be noted that in the results

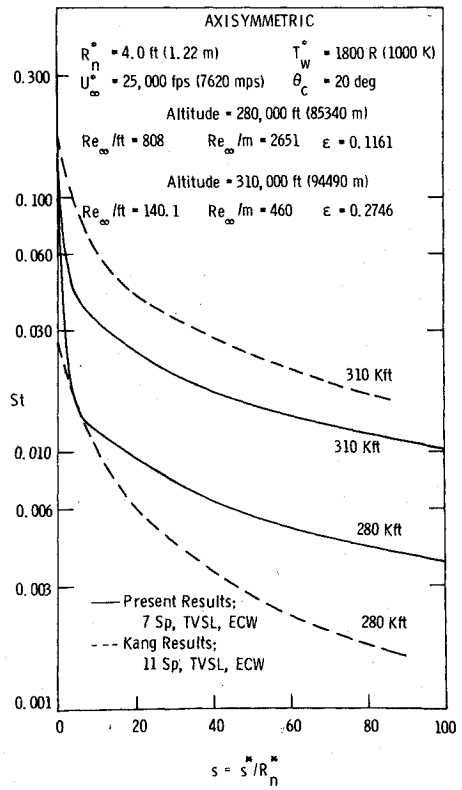


**Fig. 7 Stanton number distributions for 20° sphere cone.**

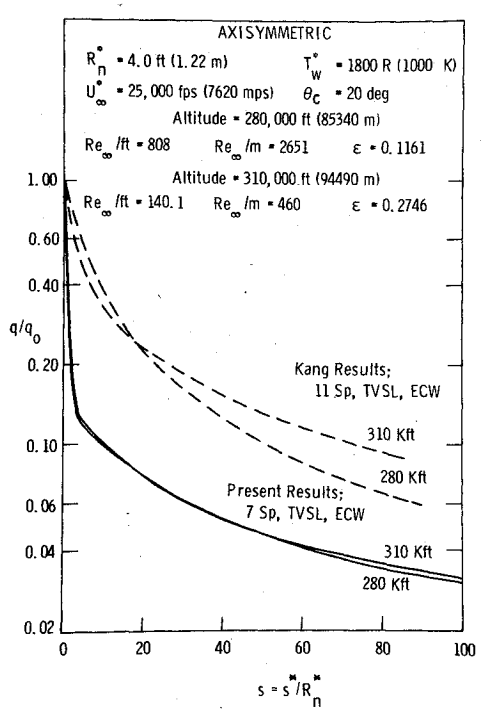


**Fig. 8 Normalized heat-transfer distributions for 20° shpere cone.**

of Tong the shock shape data used were for a different body and that entropy-layer swallowing effects are strongly dependent upon the shock shape. In the present method an initial shock shape was assumed and then updated after each global iteration. For this geometry the shock shapes from the second and third global iterations were essentially identical. A major advantage of the viscous shock-layer approach over the boundary-layer approach is evident from these results. For the viscous shock-layer approach, the shock shape is self-correcting with global iteration, and problems such as displacement-thickness interaction and shock-generated ex-

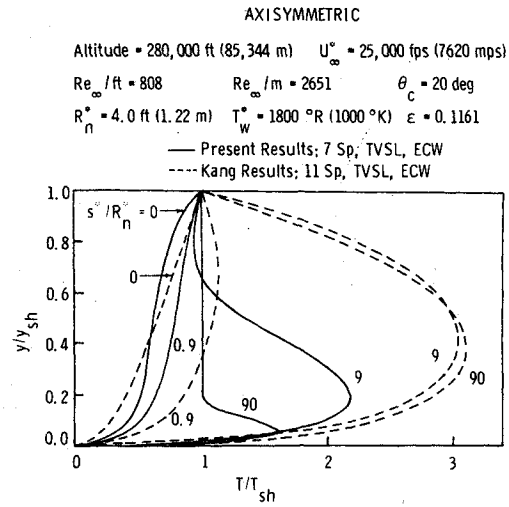


**Fig. 9 Temperature profiles for 20° sphere cone at 280,000 ft.**

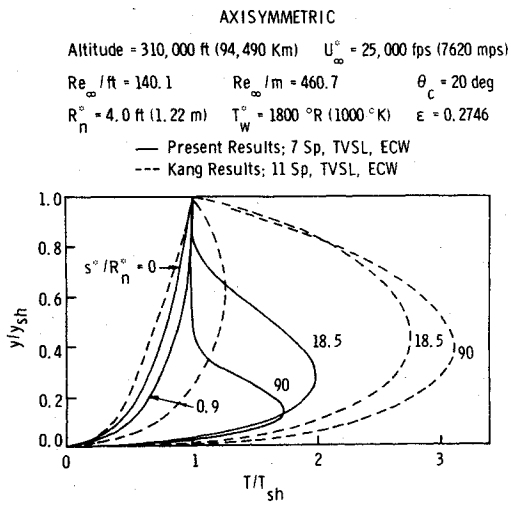


**Fig. 10 Temperature profiles for 20° sphere cone at 310,000 ft.**

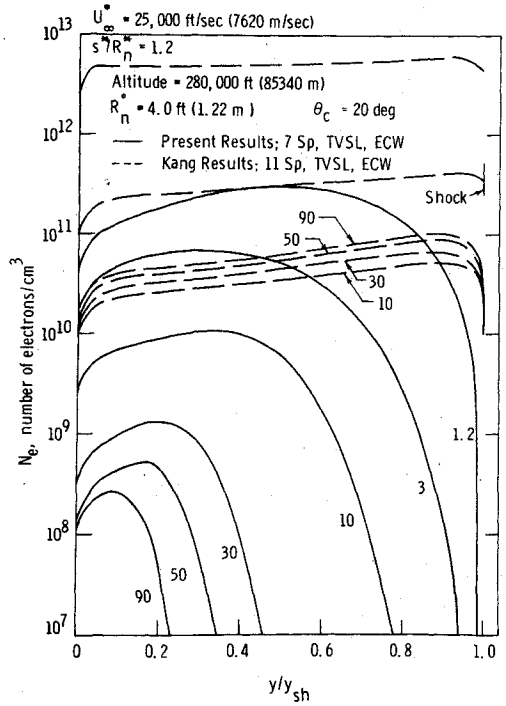


**Fig. 11 Electron concentration profiles for 20° sphere cone at 280,000 ft.**

ternal vorticity (entropy-layer swallowing and boundary-layer edge conditions) do not occur.

### 20° Sphere-Cone Case

Kang and Dunn[4-7] considered a 20° sphere cone with $R_n^* = 4$ ft as a geometry reasonably approximating the windward plane of symmetry configuration of a space shuttle. Flowfield predictions were presented for two altitudes, 280,000 and 310,000 ft. In the present work, an initial shock shape was determined for this case from a blunt body, method-of-characteristics procedure similar to that of Inouye, Rakich, and Lomax.[23] The initial shock shape was used for the first global iteration (solution for the full length of the sphere cone), and for subsequent global iterations, the shock shape was updated from the body angle and the smoothed distribution of $y_{sh}$ from the previous global iteration. Also, for this case, the predictions of the present method were made for TVSL flows, so the results would be more comparable with the results of the integral method of Kang and Dunn which were for TVSL flows only.

Predicted Stanton number distributions are shown in Fig. 7. The present results showed a significant effect of altitude on the predicted heat-transfer distributions, but the effect was less than that shown by the results of Kang and Dunn. Also, in the present predictions, the slope of the heat-transfer distribution curves changed more noticeably near the sphere-cone tangent point than in the results of Kang and Dunn. This is more apparent in the normalized heat-transfer distributions shown in Fig. 8. Also, as shown in Fig. 8, the present predictions were nearly the same for the two altitudes. The heat-transfer rates decreased rapidly as the flow expanded over the spherical nose of the body and then decreased more gradually over the conical portion. The results of Kang and Dunn showed a less pronounced decrease over the spherical nose.

Temperature profiles are shown in Fig. 9 for 280,000 ft and in Fig. 10 for 310,000 ft. The present results show that, for $s = 0$, most of the heating in the shock layer comes from the shock crossing, and that downstream more of the heating is caused by the viscous effects in the shock layer near the body. The present temperature profiles for $s = 0$ in Figs. 9 and 10 show that for 280,000 ft there is a stronger temperature

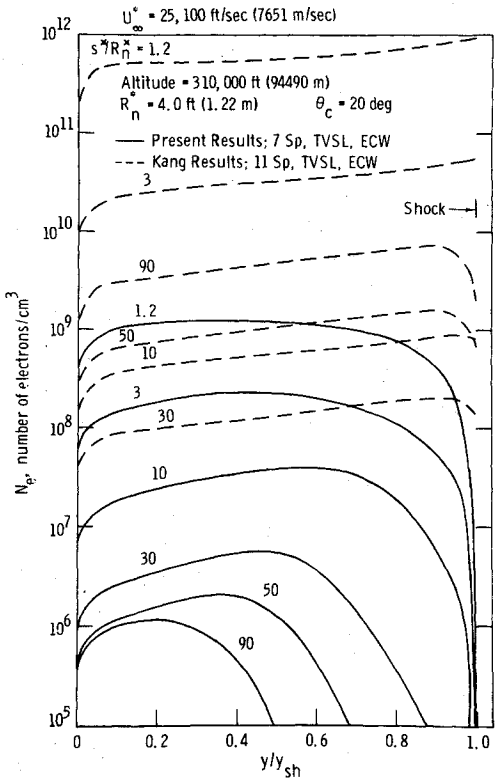


**Fig. 12 Electron concentration profiles for 20° sphere-cone at 310,000 ft.**

gradient behind the shock than for 310,000 ft, thus indicating a lower density at 310,000 ft. The downstream temperature profiles, for $s=9$, 18.5, and 90, predicted by the present method, also clearly show a thicker viscous layer at 310,000 ft than at 280,000 ft. The present results also show a downstream "recovery" of a thin boundary layer with a less rapid recovery for 310,000 than for 280,000 ft.

As noted previously for the NASA shuttle geometry case, the heat transfer predicted by the present method for dissociating oxygen and for seven species of air agreed well for the ECW condition. While not show in the present paper, for the 20° sphere-cone case, the present predictions for multicomponent air agreed well with the predicted heat-transfer distributions and temperature profiles of the present method for dissociating oxygen.

Predictions of electron concentration profiles were also made with the present method using reaction rate constants matched to those of Kang and Dunn.[4-7] The present predictions of the electron concentration profiles are shown in Figs. 11 and 12 for 280,000 and 310,000 ft. respectively. In contrast to the predictions of Kang and Dunn, the present predictions of $N_e$ show a monotonic decrease with increasing $s$. Also, the present method predicted the peak electron density in the viscous layer near the body, and much fuller electron density profiles (especially downstream) at 310,000 ft than at 280,000 ft. Thus, for the electron density profiles as well as the temperature profiles, the present viscous shock-layer method predicted an altitude effect which seems entirely reasonable and correct.

## Conclusions

The results of the present finite-difference method for predicting hypersonic viscous shock-layer flows of nonanalytic blunt bodies compared well with the boundary-layer predictions including entropy-layer swallowing of Tong, Buckingham, and Morse, for the windward plane of symmetry of a space shuttle orbiter configuration at 224,000 ft. For the low Reynolds number flows over a 20° sphere cone, a pseudo-shuttle configuration, at 280,000 and 310,000 ft, the predictions of the present method appeared quite reasonable. Also, the altitude effects of the temperature and electron concentration profiles were correctly predicted by the present method as was the "recovery" of a thin boundary layer over the downstream portion of the sphere-cone.

The present viscous shock-layer method, accurate to the second order in the Reynolds parameter $\epsilon$ eliminates most of the problems encountered in applying boundary-layer theory to hypersonic, low Reynolds number flows over nonanalytic blunt bodies such as the space shuttle orbiter. While the two cases presented here are perhaps limited in scope, the present predictions for these cases indicate the appropriateness of the present method for predicting the low Reynolds number flows for the windward plane of symmetry of the space shuttle orbiter. Further work is in progress to compare the predictions of this method with available Mach 8 wind-tunnel data for pressure and heat-transfer distributions along the orbiter windward plane of symmetry, and further predictions of the viscous flowfield are being made for the shuttle orbiter under free-flight re-entry conditions.

## References

[1] Kutler, P., Warming, R.F., and Lomax, H., "Computation of Space Shuttle Flowfields Using Noncentered Finite Difference Schemes," *AIAA Journal*, Vol. 11, Feb. 1973, pp. 196-204.

[2] Kutler, P., Reinhardt, W.A., and Warming, R.F., "Multishocked, Three-Dimensional Supersonic Flowfields with Real Gas Effects," *AIAA Journal*, Vol. 11, May 1973, pp. 657-664.

[3] Tong, H., Buckingham A.C., and Morse, H.L., "Nonequilibrium Chemistry Boundary-Layer Integral Matrix Procedure," Rept. 73-67, July 1973, Aerotherm/Acruex Corp., Mountain View, Calif.

[4] Kang, S.-W. and Dunn, M.G., "Hypersonic Viscous Shock Layer with Chemical Nonequilibrium for Spherically Blunted Cones," *AIAA Journal*, Vol. 10, Oct. 1972, pp. 1361-1362.

[5] Kang, S.-W., Jones, W.L., and Dunn, M.G., "Theoretical and Measured Electron-Density Distributions at High Altitudes," *AIAA Journal*, Vol. 11, Feb. 1973, pp. 141-149.

[6] Kang, S.-W. and Dunn, M.G., "Hypersonic Viscous Shock Layer with Chemical Nonequilibrium for Spherically Blunted Cones," TR-AF-3093-A-1, Feb, 1972, Cornell Aeronautical Lab., Ithaca, N.Y.

[7] Dunn, M.G. and Kang, S.-W., "Theoretical and Experimental Studies of Reentry Plasmas," NASA CR-2232, April 1973.

[8] Davis, R.T., "Numerical Solution of the Hypersonic Viscous Shock-Layer Equations," *AIAA Journal*, Vol. 8, May 1970, pp. 843-851.

[9] Davis, R.T., "Hypersonic Flow of a Chemically Reacting Binary Mixture Past a Blunt Body," AIAA Paper 70-805, Los Angeles, Calif., 1970.

[10] Miner, E.W. and Lewis, C.H., "Hypersonic Ionizing Air Viscous Shock-Layer Flows over Sphere Cones," *AIAA Journal*, Vol. 13, Jan. 1975, pp.80-88.

[11] Browne, W.G., "Thermodynamic Properties of Some Atoms and Atomic Ions," MSD Engineering Physics TM2, General Electric Co., Philadelphia, Pa.

[12] Browne, W.G., "Thermodynamic Properties of Some Diatomic and Linear Polyatomic Molecules," MSD Engineering Physics TM3, General Electric Co., Philadelphia, Pa.

[13] Browne, W.G., "Thermodynamic Properties of Some Diatoms and Diatomic Ions at High Temperature," MSD Advanced Aerospace Physics TM8, General Electric Co., May 1962, Philadelphia, Pa.

[14] Blottner, F.G., "Nonequilibrium Laminar Boundary-Layer Flow of Ionized Air," Rept. R64SD56, Nov. 1964, General Electric Co., Philadelphia, Pa.

[15] Miner, E.W. and Lewis, C.H., "Hypersonic Ionizing Air Viscous Shock-Layer Flows over Nonanalytic Blunt Bodies," NASA. CR-2550, May 1975.

[16] Miner, E.W. and Lewis, C.H., "Computer User's Guide for a Chemically Reacting Viscous Shock-Layer Program," NASA CR-2551, May 1975.

[17] Anderson, E.C. and Lewis, C.H., "Laminar or Turbulent Boundary-Layer Flows of Perfect Gases or Reacting Gas Mixtures in Chemical Equilibrium," NASA CR-1893, Oct. 1971; also *International Journal for Numerical Methods in Engineering*, Vol. 17, 1973, pp. 3-15.

[18] Lewis, C.H., Anderson, E.C., and Miner, E.W., "Nonreacting and Chemically Reacting Turbulent Boundary-Layer Flows," AIAA Paper 71-597, Palo Alto, Calif., 1971.

[19] Lewis, C.H., Adams, J.C., and Gilley, G.E., "Effects of Mass Transfer and Chemical Nonequilibrium on Slender Blunted-Cone Pressure and Heat-Transfer Distributions at $M_\infty = 13.2$," TR-68-214, Dec. 1968, Arnold Engineering Development Center, Tullahoma, Tenn.

[20] Lewis, C.H. and Miner, E.W., "Stagnation Point Viscous Layers with Mass Transfer," *Computers and Fluids*, Vol. 2, Aug. 1974. pp. 117-143.

[21] Evans, J.S., Schexnayder, C.J., Jr., and Huber, P.W., "Boundary-Layer Electron Profiles for Entry of a Blunt Slender Body at High Altitudes," NASA TN D-7332, July 1973.

[22] Pappas, C.C. and Lee, G., "Heat Transfer and Pressure on a Hypersonic Blunt Cone with Mass Addition," *AIAA Journal*, Vol. 8, May 1970, pp. 954-956.

[23] Inouye, M., Rakich, J., and Lomax, H., "A Description of Numerical Methods and Computer Programs for Two-Dimensional and Axisymmetric Supersonic Flow over Blunt Nosed and Flared Bodies," NASA TN D-2970, Aug. 1965.